Human-induced changes in US biogenic volatile organic compound emissions: evidence from long-term forest inventory data

D R E W   W .   P U R V E S *, J O H N   P .   C A S P E R S E N †, P A U L   R .   M O O R C R O F T ‡, G E O R G E   C .   H U R T T §
and S T E P H E N   W .   P A C A L A *
*Department of EEB, Princeton University, Princeton, NJ 08540, USA, †Faculty of Forestry, University of Toronto, 33 Willcocks Street, Toronto, ON, Canada M5S 3B3, ‡Department of OEB, Harvard University, 22 Divinity Avenue, Cambridge, MA 02138, USA, §Institute for the Study of Earth, Oceans and Space, University of New Hampshire, 39 College Road, Durham, NH 03824-3525, USA

Abstract

Volatile organic compounds (VOCs) emitted by woody vegetation influence global climate forcing and the formation of tropospheric ozone. We use data from over 250 000 re-surveyed forest plots in the eastern US to estimate emission rates for the two most important biogenic VOCs (isoprene and monoterpenes) in the 1980s and 1990s, and then compare these estimates to give a decadal change in emission rate. Over much of the region, particularly the southeast, we estimate that there were large changes in biogenic VOC emissions: half of the grid cells ($1° \times 1°$) had decadal changes in emission rate outside the range -2.3% to $+16.8\%$ for isoprene, and outside the range 0.2–17.1% for monoterpenes. For an average grid cell the estimated decadal change in heatwave biogenic VOC emissions (usually an increase) was three times greater than the decadal change in heatwave anthropogenic VOC emissions (usually a decrease, caused by legislation). Leaf-area increases in forests, caused by anthropogenic disturbance, were the most important process increasing biogenic VOC emissions. However, in the southeast, which had the largest estimated changes, there were substantial effects of ecological succession (which decreased monoterpene emissions and had location-specific effects on isoprene emissions), harvesting (which decreased monoterpene emissions and increased isoprene emissions) and plantation management (which increased isoprene emissions, and decreased monoterpene emissions in some states but increased monoterpene emissions in others). In any given region, changes in a very few tree species caused most of the changes in emissions: the rapid changes in the southeast were caused almost entirely by increases in sweetgum (*Liquidambar styraciflua*) and a few pine species. Therefore, in these regions, a more detailed ecological understanding of just a few species could greatly improve our understanding of the relationship between natural ecological processes, forest management, and biogenic VOC emissions.

Keywords: Biogenic hydrocarbons, FIA (forest inventory and analysis), forest management, land use, plantation forestry, ozone precursors

Received 12 November 2003; received in revised form and accepted 23 January 2004

Introduction

Volatile organic compounds (VOCs) emitted by vegetation are important chemical species that affect the oxidative capacity of the troposphere (NRC, 1991; Seinfeld & Pandis, 1998), and the concentrations of some chemical species that are important in climate

forcing, including CO, methane, and aerosols (Andreae & Crutzen, 1997; Mäkelä *et al.*, 1997; Hayden, 1998; Leaitch *et al.*, 1999; Shallcross, 2000; Collins *et al.*, 2002). Biogenic VOCs (BVOCs) are also precursors for tropospheric (surface-level) ozone (O_3) (NRC, 1991), which has well-documented impacts on human health and agricultural productivity. O_3 is formed by the photochemical oxidation of VOCs in the presence of NO_x (Jacob, 1999); hence, O_3 production is sensitive to emission rates of both VOCs, which have both

Correspondence: D. W. Purves, tel. $+1$ 609 258 6886, fax $+1$ 609 258 6818, e-mail: dpurves@princeton.edu

anthropogenic and biogenic sources, and NO_x, which is mostly anthropogenic (EPA, 2000; Wang & Shallcross, 2000). However, the interactions between O_3 precursors are highly nonlinear (NRC, 1991; Roselle, 1994; Jacob, 1999; Sillman, 1999; Kang *et al.*, 2003), and are affected by transport processes (Hesstvedt *et al.*, 1978), meteorology (NRC, 1991), and the differential reactivity of different VOC compounds (Seinfeld & Pandis, 1998). O_3 concentrations are also affected by regional background O_3, which is not well quantified, and that is known to be affected by long-distance transport of O_3 and its precursors (Fiore *et al.*, 2002)

In the eastern US, the total annual BVOC emissions are estimated to exceed the total annual anthropogenic VOC (AVOC) emissions (Kinnee *et al.*, 1997; Pierce *et al.*, 1998; Fuentes *et al.*, 2000; Guenther *et al.*, 2000), and adding BVOC emissions to models that already include AVOC emissions causes substantial increases in predicted O_3 concentrations (Roselle, 1994, Horowitz *et al.*, 1998, and Pierce *et al.*, 1998: although in areas with low NO_x levels the effect can be opposite: Roselle, 1994). However, modelling studies have assumed that US BVOC emissions are static on the decadal timescales relevant to air pollution policy. Research into trends in BVOC emissions has concentrated on climate change, which can affect BVOC emissions directly because leaf-level emission rates depend on temperature and light, and indirectly by changing vegetation (Constable *et al.*, 1999; and at a global scale Sanderson *et al.*, 2003). The changes in emissions predicted for recent decades have been small, because climate changes have been small, and because the equilibrium vegetation models used in these studies assume that current vegetation has reached a steady state with respect to current climate, which precludes the possibility of significant recent changes.

However, there are likely to have been significant changes in US emissions of BVOCs over timescales of decades and centuries, independent of climate change (Monson *et al.*, 1995; Lerdau & Slobodkin, 2002). The historical pattern of de-forestation followed by re-forestation in the eastern US (Hurtt *et al.*, 2002) must have produced a pronounced decrease and subsequent increase in emission rates, because woody vegetation emits orders of magnitude more O_3-forming VOC than non-woody vegetation (Guenther *et al.*, 1994; Kesselmeier & Staudt, 1999; Fuentes *et al.*, 2000). Changes in species composition within forests could also have resulted in substantial BVOC emission changes, for two main reasons. First, different species emit greatly different amounts of BVOC. For example, under identical conditions an equal leaf area of Quaking Aspen (*Populus tremuloides*) is predicted to emit isoprene at ca. 650 times the rate of Eastern Hemlock

(*Tsuga canadensis*), and no isoprene emission has been detected from any US Maple (*Acer* species). Second, the variation in emission rate is correlated with ecological characteristics (Harley *et al.*, 1999). For example, within deciduous trees, the highest emitters are shade-intolerant and early-successional (e.g. Aspens, Poplars, Sweetgum) and late-successional broadleafs tend not to emit at all (e.g. Beech, Sugar Maple), and the chemical species emitted by broadleafs tends to be isoprene, compared with monoterpenes for conifers, although there are exceptions to these patterns (e.g. Spruce emits isoprene). Also potentially important is the recent increase in plantation forestry (Zhou *et al.*, 2003), which usually uses tree species that are high emitting for BVOC (e.g. Poplars, Eucalypts, Pines).

We estimate a decadal change in eastern US BVOC emissions between the 1980s and 1990s, caused by changes in the extent, structure, and species composition of forests. Our estimate is given by the most widely used leaf-level emissions model (from Guenther *et al.*, 1993), in conjunction with the USDA Forest Service Inventory Analysis (FIA) forest inventory, which recorded vegetation changes in over 250 000 re-surveyed forest plots in the region. The changes themselves (e.g. tree growth, ecological succession) are not modelled, but observed: therefore, our estimate of systematic changes in emissions results entirely from systematic changes in the inventory data. We hold climate constant, confining attention to changes in the extent, structure, and composition of forests. Finally, we decompose the changes in BVOC emissions into different processes (harvesting, ecological succession, leaf-area change, plantation management, de- and re-forestation), and different tree species.

The results indicate substantial recent increases in eastern US BVOC emissions, especially in the south of the region. This result has potentially important implications for air-quality policy, but in relating our results to air pollution, there are some crucial points that should be kept in mind. First, nearly all NO_x is anthropogenic, and without this pollution, O_3 concentrations would probably never reach high enough concentrations to affect human health or agricultural productivity (e.g. Wiedinmyer *et al.*, 2000). Second, in a low-NO_x chemical regime, as would exist in the US without anthropogenic NO_x emissions, VOCs act to decrease, rather than increase, O_3 concentrations (Roselle, 1994; Mickley *et al.*, 2001). Third, our analysis suggests that over much of the region, legislated decreases in AVOC emissions were masked by approximately equal increases in BVOC emissions, which may help to explain why the AVOC emission reductions did not lead to a general reduction in O_3 (e.g. Lin *et al.*, 2001); therefore, this legislation may have been more

successful than previously thought, since O_3 concentrations may be lower now than they would have been without the legislation. Fourth, we estimate that BVOC emissions in the eastern US are large compared with AVOC emissions (as has been found previously), and are increasing, both of which suggest that in general reducing anthropogenic emissions of NO_x, rather than anthropogenic or biogenic VOCs, would be the most effective means of reducing O_3 concentrations in the future. Fifth, it is nevertheless important to acknowledge that BVOC emissions are a part of the US O_3 problem, because they are known to contribute to O_3 when sufficient NO_x is available (as is currently the case for the eastern US), because they are changing rapidly with respect to other precursors, and because the changes in BVOC emissions mostly result from anthropogenic disturbances anyway. The results reported here call for a wider recognition that an understanding of recent, current, and anticipated changes in biogenic VOC emissions is necessary to guide future air-quality policy decisions; they do not provide any evidence that responsibility for air pollution can or should be shifted from humans to trees (Reagan, 1980).

Methods

Our estimate of BVOC emissions, and emission changes, was based on the USDA FIA database, which contains detailed information on the species composition and management of over 250 000 forest plots in the eastern US. The plots were surveyed once in the 1980s, and again in the 1990s; thus, it was possible to observe changes in forest structure and composition that occurred between the surveys. We use a standard BVOC emission modelling technique with the 1980s data, and then separately with the 1990s data, to estimate changes in emissions. Therefore, although estimating BVOC emissions necessarily involves a number of modelling steps, the model does not contain any representation of dynamical processes such as growth, species compositional change, or changes in land use: these dynamics are observed in the inventory data. Therefore, without systematic change in the inventory data, there would have been no systematic change in the estimated BVOC emission rates.

FIA data

The FIA for the eastern US, for this time period, gives data from forest inventory plots that were surveyed once in the 1980s, and again in the 1990s, with the exact years differing from state to state. Inventories were performed separately for each state and followed a two-phase sampling procedure known as double sampling

for stratification. In the first phase, a random sample of points was located on aerial photographs and was classified by land cover and forest type. In the second phase, a random subsample of the photo points was selected from each of the classes, located on the ground, and established as a field plot. For each field plot, a number of variables were recorded, including current land use, previous land use, stand age, and plantation vs. natural forest. Within each forested plot, trees were sampled from a cluster of five or more points. Trees 1–5 in in diameter were sampled from a fixed-radius circular area around each point. Larger trees were sampled using variable radius plot sampling, which in effect uses a larger circular plot for larger trees, and is an efficient method for estimating plot basal area and wood volume (Hansen *et al.*, 1992). For each tree sampled, a number of observations were recorded, including species, status (live, dead from harvesting, dead from natural causes), and diameter at breast height (dbh). The volume of data in the FIA for this period is extremely unusual for an ecological dataset. For this region, there were over 250 000 resurveyed field plots with measurements and re-measurements of over 2.7 million trees.

The FIA methodology was designed specifically to provide accurate estimates of regional (county or state level) characteristics. The field sampling enables the estimation of average forest characteristics (e.g. tree density, average tree size, species composition) and changes in these characteristics (e.g. increment in wood volume). The aerial photographic data enable these characteristics to be scaled up to the regional level, by calculating the fraction of the land surface belonging to each of the different classes of land-use and forest type. Both parts of this procedure are included in the results we present here; thus for example, VOC emissions and changes in emissions are lower in locations with a lower forest cover.

Our estimate of systematic changes in VOC emissions results entirely from systematic changes observed in the FIA data. To examine these changes separately from the detailed predictions of the VOC emission model, we first classified each North American tree species as an emitter or non-emitter for both isoprene and monoterpene, based on species-specific VOC emission measurements (Appendix), and calculated the mid-1980s standing basal area, and the decadal change in basal area, for isoprene emitters and monoterpene emitters for each $1° \times 1°$ grid cell (Fig. 1, Appendix).

Uncertainty in the FIA data reflects a number of potential sources of error including the measurement of individual tree sizes and the estimates of forest area from aerial photography, but the total uncertainty is dominated by sampling error at the plot level (Phillips

et al., 2000). The errors in calculations based on FIA data are low, with decadal changes at the county level (areas approximately the same as our 1×1 grid cells) estimated to within 5% (Phillips *et al.*, 2000). Also, because the FIA surveyed the same plots in both survey periods, so that most individual trees are measured twice, the sampling error is highly correlated in time (for example plots with a high density of trees at time 1 also do so at time 2). This correlation means that when calculating changes much of the error cancels, leaving an estimate for the change that is much more accurate than might be expected from the uncertainty in the estimates of absolute values rate at any one time (Appendix). This property carries through the BVOC emission model, so that the data uncertainty in the estimate of BVOC emission changes (Fig. 3) is less than the data uncertainty in the estimate for BVOC emissions at any one time (Fig. 2).

BVOC emission model. We estimate BVOC emissions from the FIA data in five steps. First, we assign a potential emission rate (per unit leaf area) to each species listed in the FIA database based on field measurements. Second, we estimate the spatial distribution of leaf area for each tree using a simple empirical canopy model, and allometries parameterized from field studies. Third, using the widely used leaf-level emissions algorithms given in Guenther *et al.* (1993), we estimate the VOC emission rates for each tree canopy on a standard hot bright day (air temperature 35 °C, incoming short-wave radiation 1000 W m^{-2}). Heatwave emissions are important for the peak O$_3$ events that are most important for air quality, which is why we report heatwave results here. Fourth, we aggregate the tree-level emissions to obtain an emission rate, and a decadal change in emission rate, for each inventory plot, and thus for each $1° \times 1°$ grid cell, in the eastern US. Fifth, we decompose changes in BVOC emissions into the contributions from different processes and different species. Throughout, we adopt a minimal complexity approach to the modelling: additional processes that are known to occur, and that have been incorporated into other emission inventories, are only included if the available data are sufficient to imply more accurate estimates for heatwave emission rate.

The accuracy of the estimates of BVOC emissions at any one time, and the estimates of decadal changes in emissions, is affected by two different types of uncertainty: uncertainty in the FIA data (data uncertainty), and model uncertainty, which reflects both the basic assumptions of the model and the parameter values used for different functions. However, when calculating a change, differences in many assumptions and parameters will increase or decrease emission estimates at both survey times, and thus will tend to cancel. As a result, models with different assumptions can give significantly different estimates for absolute emission rates at one time, but similar estimates for the changes in emissions between survey times (this is a general property of such models). To address some of the issues regarding model uncertainty, we try six alternative models that differ in assumptions about the behaviour of tree crowns and forest canopies (models B1–C3). We find that the change estimate is highly robust, with five models giving almost identical estimates. The estimates for absolute emissions are more variable, but are close to previous estimates for this region. There are other important uncertainties that may have a significant impact on the estimates of changes in emissions, most notably the species-specific parameters for leaf characteristics, allometries, and potential emission rates. Analysis of the contribution to the total model error from uncertainty in these parameters is complicated because they all interact nonlinearly. The model predictions are also difficult to verify because of a lack of direct measurements of BVOC fluxes (see the Discussion). For this reason, the quantitative estimates should be viewed as an indication of the magnitude and spatial distributions of BVOC emissions, changes in BVOC emissions, and the relative magnitude of biogenic vs. anthropogenic emissions and emission changes.

Species-specific potential emission rates

Each tree was assigned a potential emission rate for isoprene and monoterpenes, $E_{\text{iso}}^{(i)}$ and $E_{\text{mono}}^{(i)}$ (mg m^{-2} h^{-1}) based on its species. The species-specific emission rates were taken from a public-access database made available by Hope Stewart and colleagues (http://www.es.lancs.ac.uk/cnhgroup/iso-emissions.pdf and see Stewart *et al.*, 2003). which gives potential emissions as VOC emission rate per unit dry mass of leaf (μg g^{-1} h^{-1}). We converted these values to emission rate per unit leaf area per hour (mg m^{-2} h^{-1}) using a value for SLA (area of leaf per unit leaf dry mass) specific to each species (see White *et al.* (2000) and for the origin of the SLA values, to be stated).

Species with no available emission measurement were assigned the average value for eastern North American species within that genus: if no rate was available from the same genus, the rate was set at zero. For isoprene and monoterpenes, respectively, 65% and 45% of individual trees received a species-specific emission rate, and only 0.8% and 8.1% had no available species- or genus-specific value. Within some genera

(e.g. Oaks), there is significant species-specific variation in emission rates, which means that assigning genus averages could be problematic, but this cannot be tested directly because the measurements are not available. However, many genera have little within-genus variation in emission rates.

Spatial distribution of leaf area

Estimating emissions for each tree requires a model of the tree canopy, the minimum requirements for which are a potential emission rate per unit leaf area, the spatial distribution of leaf area, and the light and temperature conditions to which each leaf layer is subjected (to be described). Leaves shade each other, causing a decaying profile of light down through the canopy, which in turn causes a vertical gradient in temperature. It therefore matters whether the total leaf area is arranged in a wide crown, giving a low leaf-area index (LAI) (= area of leaf/area of canopy, low LAI means little shading of leaves); or in a narrow crown, giving a high LAI (and thus highly shaded leaves and lower emissions). The crown area and the total leaf area of each tree specify the spatial distribution of leaf area.

There are two major uncertainties in this approach: both crown area and total leaf area are likely to vary with stand density. This will be explained, along with the methods we used to calculate canopy area and leaf area. The methods that we use are not the only possible ones, and alternative methods for calculating canopy area and leaf area could give estimates of emissions that differ from those presented in Fig. 1; however, we did examine sets of alternative assumptions and these gave very similar change estimates. Therefore, the BVOC change estimates appear to be robust to these assumptions. The results presented in Figs 2 and 3 were generated using what we believe to be the most appropriate choice of assumptions, given the information currently available.

Crown area. The crown area (vertical projection of the crown onto the ground) of each individual tree was predicted from dbh using an empirically derived allometric function given in a forest model (Pacala *et al.*, 1996):

$$c^{(i,t)} = \pi[\rho \, \mathrm{dbh}^{(i,t)}]^2, \tag{1}$$

where $c^{(i,t)}$ is the crown area (m^2) of tree i, dbh$^{(i,t)}$ is the diameter at breast height (cm), and ρ scales dbh$^{(i,t)}$(cm) to the canopy radius (m). We use the average ρ for broadleafs (0.115) and conifers (0.094) given in Pacala *et al.* (1996). The total canopy area of plot j at time t, $C^{(j,t)}$(ha ha^{-1}), was then calculated as a weighted sum of the areas of the individual tree crown areas:

$$C^{(j,t)} = 10^{-4} \sum_{\{i \in R(j)\}} w^{(i)} c^{(i,t)}, \tag{2}$$

where $w^{(i)}$ is the tree expansion factor, and the set $R(J)$ contains all measured trees within plot j (some trees are excluded from the analysis). Eqn (2) is free to predict that $C^{(j,t)} > 1.0$(i.e. total crown area exceeding ground area), in which case one must either (A) allow adjacent canopies to interdigitate, and run the canopy model with a mixed canopy of different species or (B) reduce canopy sizes to keep $C^{(j,t)}$ below or equal to 1.0. Method A would be difficult to implement and the necessary data for doing so are not available, and interdigitating crowns are almost never observed in reality, beyond a very narrow region at the canopy edges. We therefore adopted method B when $C^{(j,t)}$ exceeded 1.0, by applying the transformation

$$c^{(i,t)} \Rightarrow c^{(i,t)}(1/C^{(j,t)}). \tag{3}$$

Applying Eqn (3) forces the total canopy area to equal the ground area ($C^{(j,t)} = 1.0$), and implies that the trees have adjusted their crown widths to keep the canopy exactly filled without interdigitating. It is possible that plasticity in growth also operates when the canopy is underfilled, i.e. where $C^{(j,t)} < 1.0$ trees may widen their crowns to fill the canopy. Thus, we tested an alternative method (C) that assumes that the canopy is always perfectly filled in every plot. Method C was implemented by applying transformation Eqn (3) to every plot, regardless of $C^{(j,t)}$ prior to transformation. Method B was used to obtain the emissions estimates we derived, but method C was also implemented to determine whether alternative assumptions have a significant effect on the results.

Leaf area. An allometric approach was also used to predict leaf mass and leaf area:

$$m^{(i,t)} = \phi[\mathrm{dbh}^{(i,t)}]^\sigma, \tag{4}$$

where $m^{(i,t)}$ is the leaf mass (g) of tree i at time t, and ϕ and σ are empirical coefficients. The values of ϕ and σ were taken from Ter-Mikaelian & Korzukhin (1997), which gives several values of ϕ and σ for 65 North-American species (several values because there have been several studies for some species: ϕ and σ are given as a and b in Ter-Mikaelian & Korzukhin, 1997). We selected one pair of ϕ and σ for each species by selecting the study with the highest value of n range^2, where n is the number of trees used to fit the function, and range is the range of dbh values used to fit the function (in many cases, this choice was moot because only one study was available, and in many other cases the parameters from different studies were very

similar). Species not covered in Ter-Mikaelian & Korzukhin (1997) were given genus-level average values for ϕ and σ, and species with no congeneric allometry were given the averages for broadleafs or conifers.

Leaf mass was converted to leaf area using an SLA value (cm^2 leaf area g^{-1} leaf mass) taken from White et al. (2000), which gives one or more SLA values for many North-American species (as m^2 kg (carbon): the conversion to cm^2 g (drymass) is $\times 5.0$). Species covered by White et al. (2000) were given the average SLA for the species; species not covered were given a genus or broadleaf/conifer average, as described for ϕ and σ. The SLA values were used to calculate the leaf area of each tree $a^{(i,t)}$ (m^2) from total leaf mass

$$a^{(i,t)} = m^{(i,t)} \, SLA^{(i)}. \qquad (5)$$

LAI was then calculated as the ratio of total leaf area to crown area

$$LAI^{(i,t)} = a^{(i,t)}/c^{(i,t)}. \qquad (6)$$

Eqns (4–6) imply that a tree of a given size can adopt a higher LAI in a more crowded stand, because leaf area depends only on dbh$^{(i,t)}$, but canopy area is reduced when $C^{(j,t)}$ exceeds 1.0. In some cases, this could lead to unrealistically large LAI (beyond a certain LAI an extra layer of leaves becomes a net sink, rather than a source, of carbohydrate; thus very large LAI values are not observed). To assess the potential importance of this, and to correct any problems, we use alternative methods to estimate leaf area: (1) using the allometric approach (Eqns (4–6)); (2) using the allometric approach, but limiting the LAI of any tree to 6.0; and (3) using a constant LAI of 6.0 for all trees, regardless of dbh or the sizes of other trees in the plot. Thus, in combination with the two methods for normalizing crown area, there are six alternative methods for estimating the spatial distribution of leaf area (Table 1).

Leaf-level emission algorithms

The potential emission rates $E_{iso}^{(i)}$ and $E_{mono}^{(i)}$ described are defined as the emission rate per unit leaf area, for a leaf at 30 °C, with an incoming PAR of 1000 μmol m^{-2} s^{-1}. The Guenther et al. (1993) algorithms predict leaf-level emission rates at any given temperature and incoming radiation from these potential values. Following the recommendations in Guenther et al. (1993) we use 'G93' to model isoprene, and Eqn (5) in Guenther et al. (1993) to model monoterpenes. The total emissions of the canopy are calculated as the sum of leaf-layer emissions, over the multilayered canopy (each tree has a separate canopy). The methodology is close to that used to estimate actual emissions for forest stand canopies in the BEIS-2 model (Pierce et al., 1998).

Isoprene. At time t, an estimated canopy-level actual emission rate for isoprene $I_{iso}^{(i,t)}$ (mg m^{-2} h^{-1}) is calculated as an integral over L, the cumulative LAI of the canopy (L is equal to zero at the top of the canopy)

$$I_{iso}^{(i,t)} = \int_0^{L_{max}} E_{iso}^{(i,t)} f_{iso}^{temp}(T(L)) f_{iso}^{PAR}(PAR(L)) \, dL, \qquad (7.1)$$

$$= E_{iso}^{(i,t)} \int_0^{L_{max}} f_{iso}^{temp}(T(L)) f_{iso}^{PAR}(PAR(L)) \, dL, \qquad (7.2)$$

where L_{max} is the total canopy LAI of the tree canopy calculated according to one of models B1–C3; $T(L)$ is the leaf temperature at cumulative LAI L; and PAR(L) is the incident radiation at cumulative LAI L. $E_{iso}^{(i)}$ can be taken outside the integral over L (Eqn (7.2)) because we hold $E_{iso}^{(i)}$ constant through the canopy. Potential emission rates have been shown in some cases to vary between sun and shade leaves (e.g. Harley et al., 1997), but at present the necessary species-specific data are not available: including this detail would tend to increase emissions because the brightest leaves would also have higher potential emissions, but it is not certain that

Table 1 Summary of differences in assumptions between alternative canopy and leaf-area models

Total plot crown area	LAI of each tree		
	From Eqn (6), unrestricted	From Eqn (6), but limited to 6.0	Fixed at 6.0
From Eqn (2), but normalized to 1.0 ha ha^{-1} where Eqn (2) predicts > 1.0 ha ha^{-1}	B1	B2	B3
Always normalized to 1.0 ha ha^{-1}	C1	C2	C3

LAI, leaf-area index.

these higher estimates would be more accurate. Potential emission rates have also been shown to depend on temperatures over several days prior to the measurement, but the temperature histories are not provided with the potential emission rate measurements; thus, this detail is not included in our model (although it could be very important in modelling short-term variation in emission rates). Finally, potential emission rates also vary with leaf age, but because leaf ages are not given with the potential emission measurements, this effect is not included in our model.

The function $f_{\text{iso}}^{\text{temp}}$ describes how isoprene emission rate depends on leaf temperature $T(L)$ (Guenther et al., 1993):

$$f_{\text{iso}}^{\text{temp}}(T(L)) = \frac{\exp\left(\frac{C_{T1}[T(L)-T_s]}{RT_sT(L)}\right)}{1 + \exp\left(\frac{C_{T2}[T(L)-T_m]}{RT_sT(L)}\right)}, \qquad (8)$$

where C_{T1}(95 000 J mol^{-1}), C_{T2}(230 000 J mol^{-1}), and T_m(314 K) are empirical coefficients; T_s is the standard temperature referred to by the potential emission values (in this case 303.15 K = 30 °C); parameter values for C_{T1}, C_{T2}, and T_m are as given in Guenther et al. (1993); and R is the universal gas constant (8.314 J K^{-1} mol^{-1}). Leaf temperature is assumed to decay exponentially from above air temperature $(T_{\text{air}} + T_{\text{diff}})$ at the top of the canopy $(L = 0)$, to equal to air temperature (T_{air}) at very large L:

$$T(L) = T_{\text{air}} + T_{\text{diff}}\, e^{-0.50L}. \qquad (9)$$

For our heatwave condition, we set $T_{\text{air}} = 35$ °C (308.15 K) and use $T_{\text{diff}} = 10$ and 2 °C for broad- and needle-leaved species, respectively. The use of a constant T_{diff} is a simplification because the difference between leaf and air temperature depends on meteorological conditions including air temperature, wind speed, and humidity. The values are reasonable for a heatwave, but a more sophisticated treatment is required to extend the model to different meteorological conditions.

The function $f_{\text{iso}}^{\text{PAR}}$ describes how leaf-level isoprene emission rate depends on the incoming radiation PAR(L):

$$f_{\text{PAR}}(\text{PAR}(L)) = \frac{\alpha C_{L1}\,\text{PAR}(L)}{\sqrt{1 + \alpha^2\,\text{PAR}(L)^2}}, \qquad (10)$$

where α (0.0027) and C_{L1}(1.066) are empirically derived coefficients given in Guenther et al. (1993). PAR for a given cumulative LAI, PAR(L) and incoming PAR P_{max}, is modelled using Beer's law with an extinction coefficient of 0.50:

$$\text{PAR}(L) = P_{\text{max}}e^{-0.50L}. \qquad (11)$$

For our heatwave condition, we set $P_{\text{max}} = 1150$ μmol m^{-2} s^{-1}, corresponding to an incoming short-wave radiation of 1000 W m^{-2}.

Monoterpenes. Following the Guenther et al. (1993) algorithms, monoterpene emission rate depends on leaf temperature but is independent of light level. As for isoprene, the canopy-level emission rate is calculated as an integral over the cumulative LAI, L:

$$I_{\text{mono}}^{(i,t)} = \int_0^{L_{\text{max}}} E_{\text{mono}}^{(i,t)} f_{\text{mono}}^{\text{temp}}(T(L))\, dL \qquad (12.1)$$

$$= E_{\text{mono}}^{(i,t)} \int_0^{L_{\text{max}}} f_{\text{mono}}^{\text{temp}}(T(L))\, dL. \qquad (12.2)$$

The function $f_{\text{mono}}^{\text{temp}}$ describes how monoterpene emission depends on leaf temperature $T(L)$:

$$f_{\text{mono}}^{\text{temp}}(T(L)) = e^{0.09[T(L)-T_s]}, \qquad (13)$$

with $T_s = 303.15$ K as before, and leaf temperature modelled by Eqn (9). The value 0.09 is an empirically derived coefficient given in Guenther et al. (1993).

Plot and grid-cell averages

Because of the sampling design of the FIA, individual tree measurements and the characteristics of individual plots, must be differentially weighted according to tree- and plot-level expansion factors, which express the values on a common per-unit area basis (Hansen et al., 1992). The tree-level expansion factor for tree i, $w^{(i)}$ (in this case ha^{-1}) is given by

$$w^{(i)} = 1/(N^{(j)}A^{(i)}), \qquad (14)$$

where $A^{(i)}$ is the area sampled (ha) for trees of the same size as i, and $N^{(j)}$ is the number of points at which trees were sampled from plot j. The FIA provides a plot-level expansion factor $w^{(j)}$ for each plot j, calculated from aerial photography, which weights the contribution of plot j to the grid-cell average.

Plot averages. The Guenther et al. (1993) algorithms gave emission rates for isoprene/monoterpene, $I_{\text{iso/mono}}^{(i,t)}$ (mg m^{-2} h^{-1}) for each tree i based on the species-specific potential emission rate $E_{\text{iso/mono}}^{(i)}$, canopy area $c^{(i,t)}$, LAI LAI$^{(i,t)}$, and environmental conditions. The plot-level emission rate $I_{\text{iso/mono}}^{(j,t)}$ (mg m^{-2} h^{-1}) was calculated as

$$I_{\text{iso/mono}}^{(j,t)} = 10^{-4} \sum_{\{i \in R(j)\}} w^{(i)} c^{(i,t)} I_{\text{iso/mono}}^{(i,t)} \qquad (15)$$

with the expansion factor $w^{(i)}$(ha^{-1}) calculated from initial (first survey) tree size (Martin, 1982). $R(j)$

contains all trees within plot j that were measured at time t, excluding trees greater than 5 in in diameter that were not measured in the first inventory (following Martin, 1982). A decadal rate of change in emission rate $\Delta I_{\text{iso/mono}}^{(j)}(\text{mg m}^{-2}\text{h}^{-1})$ was calculated for each plot j:

$$\Delta I_{\text{iso/mono}}^{(j)} = [1/\Delta t][I_{\text{iso/mono}}^{(j,t+\Delta t)} - I_{\text{iso/mono}}^{(j,t)}], \quad (16)$$

where Δt is the time interval between surveys (decades). In each case, there were two different values of $I_{\text{iso/mono}}^{(k,t)}$, one for the 1980s and 1990s, with an average Δt of 9.6 years = 0.96 decades. The value of Δt differed from plot to plot but was generally identical for plots in the same state.

Cell averages. The emission rates for grid cell k, $I_{\text{iso/mono}}^{(k,t)}(\text{mg m}^{-2}\text{h}^{-1})$ was calculated as a weighted mean of plot-level emissions:

$$I_{\text{iso/mono}}^{(k,t)} = \frac{\sum_{\{j \in R(k)\}} w^{(j)} I_{\text{iso/mono}}^{(j,t)}}{\sum_{\{j \in R(k)\}} w^{(j)}}, \quad (17)$$

where $R(k)$ contains all plots within grid cell k that had data for the FIA survey at time t. Similarly, a grid-cell level decadal rate of change $\Delta I_{\text{iso/mono}}^{(k)}(\text{mg m}^{-2}\text{h}^{-1})$ was calculated as

$$\Delta I_{\text{iso/mono}}^{(k)} = \frac{\sum_{\{j \in R_2(k)\}} w^{(j)} \Delta I_{\text{iso/mono}}^{(j)}}{\sum_{\{j \in R_2(k)\}} w^{(j)}}, \quad (18)$$

where $R_2(k)$ contained all re-measured plots (data from both FIA surveys) within grid cell k. The sets $R(k)$ and $R_2(k)$ contained plots that were non-forested at one or both survey times: plots not forested at time t were given an emission rate of zero for time t. For this reason, the grid-cell averages $I_{\text{iso/mono}}^{(k,t)}$ and $\Delta I_{\text{iso/mono}}^{(k)}$ were affected by the fraction forest cover within cell k.

Decomposing changes in BVOC emissions: processes. This section describes how the grid-cell rate of change in BVOC emissions $\Delta I_{\text{iso/mono}}^{(k)}$ was decomposed into the individual effects of five separate processes: ecological succession, $\Delta_s I_{\text{iso/mono}}^{(k)}$; harvesting, $\Delta_h I_{\text{iso/mono}}^{(k)}$; leaf-area change, $\Delta_{\text{lea}} I_{\text{iso/mono}}^{(k)}$; de- and re-forestation, $\Delta_{\text{dr}} I_{\text{iso/mono}}^{(k)}$; and plantation management, $\Delta_{\text{pm}} I_{\text{so/mono}}^{(k)}$. The decomposition allowed a comparison of the direction and magnitude of the changes that would have been caused by each process if it had acted in isolation, but because of the nonlinearity of the interactions between the different processes the sum of the separate values does not equal the total change. The grid-cell level change in emission rate induced by each process ($\Delta_x I_{\text{iso/mono}}^{(k)}$, where $x = \text{s, h, lea, dr, or plm}$) was

calculated as

$$\Delta_x I_{\text{iso/mono}}^{(k)} = \frac{\sum_{\{j \in R_x(k)\}} w^{(j)} \Delta I_{\text{iso/mono}}^{(j)}}{\sum_{\{j \in R_2(k)\}} w^{(j)}}, \quad (19)$$

where $R_2(k)$ contains all re-measured plots j within grid cell k (i.e. plots that were measured during both FIA surveys) as above, and $R_x(k)$ contains all re-measured plots that also meet a number of extra criteria specific to process x, as follows: *Succession*: plot not harvested during survey interval; plot classified as forest at both survey times; plot not classified as plantation at any survey time. *Harvesting*: plot harvested during survey interval; plot classified as forest at both survey times; plot not classified as plantation at any survey time. *Leaf-area change*: plot classified as forest at both survey times; plot not classified as plantation at any survey time. *De- and re-forestation*: plot classified as nonforested at either survey time; plot not classified as plantation at any survey time. *Plantation management*: plot classified as plantation at either survey time.

The method for calculating $\Delta I_{\text{iso/mono}}^{(j)}$ was also specific to the process. For de- and re-forestation, and plantation management, $\Delta I_{\text{iso/mono}}^{(j)}$ was calculated using method B2 from the inventory data exactly as described. For succession and harvesting, the change in emissions for plot j was calculated as the difference between the emissions at the first survey time, calculated from model B2 with the observed data from the first survey time, and the emissions at the second survey time, calculated from model B2 with alternative time-2 data for plot j. This alternative plot data had the species composition observed in plot j at time 2, but the total plot crown area and leaf area observed at time 1. Calculating change in this way restricted the change to reflect changes in species composition, with no change in crown or leaf area. For leaf-area change, the same technique was used as for succession and harvesting, but with the alternative time-2 data created by combining the species composition observed at time 1, with the total plot crown area and leaf area observed at time 2: therefore in this case the change in emissions reflected changes in crown and leaf area, with no change in species composition.

Decomposing changes in BVOC emissions: species

The total changes in emissions for two different regions were separated into the contributions of different species in different settings. This was done by first, altering the definition of the set $R(j)$ in Eqn (15) to include only those trees that, in addition to the criteria given for Eqn (15), are of the species of interest, in the

setting of interest (natural forest, pine plantation or hardwood plantation). Thus, the calculated values of $I_{\text{iso/mono}}^{(k,t)}$, and hence the values of $\Delta I_{\text{iso/mono}}^{(k)}$, represent the changes associated with one species s in one setting x only, $\Delta I_{\text{iso/mono}}^{(r,s,x)}$. Second, rather than averaging the changes at the grid-cell level (Eqn (18)), we simply summed the values of $\Delta I_{\text{iso/mono}}^{(k)}$ over one of the two regions r to produce a total change for the region $\Delta I_{\text{iso/mono}}^{(r,s,x)}$ (kg h^{-1}):

$$\Delta I_{\text{iso/mono}}^{(r,s,x)} = \sum_{\{j \in R_2(k)\}} w^{(j)} \Delta I_{\text{so/mono}}^{(j,s,x)}. \qquad (20)$$

Note that for this analysis, we did not normalize $\Delta I_{\text{iso/mono}}^{(r,s,x)}$ by the total of the plot-level expansion factors $w^{(j)}$, thus the values of $\Delta I_{\text{iso/mono}}^{(r,s,x)}$ can be compared between the two different regions in terms of their contributions to the total emissions of the eastern US. Finally, to produce Fig. 5 we used Eqns (15–16) to calculate $\Delta I_{\text{iso/mono}}^{(r,s,x)}$ for each species s, in each setting x, in each of the two regions r, for both isoprene and

monoterpenes. Then, separately for each combination of setting x, region r, and isoprene and monoterpenes, we ranked the different species s by the magnitude of the value of $\Delta I_{\text{iso/mono}}^{(r,s,x)}$, and output the results for the six most important species in each case. In no case did a species with a lower rank than 6 have a significant impact on changes in emissions.

Results

Distribution and changes in basal area

The distribution of basal area of isoprene- and monoterpene-emitting species recorded in the inventory data was heterogeneous and correlated with forest extent and species composition (Fig. 1, top). For example, the basal area of isoprene emitters was high in the Southern Appalachians and the Ozarks (southern Missouri and northern Arkansas), which have extensive Oak-dominated forests (Oaks tend to emit isoprene), and the
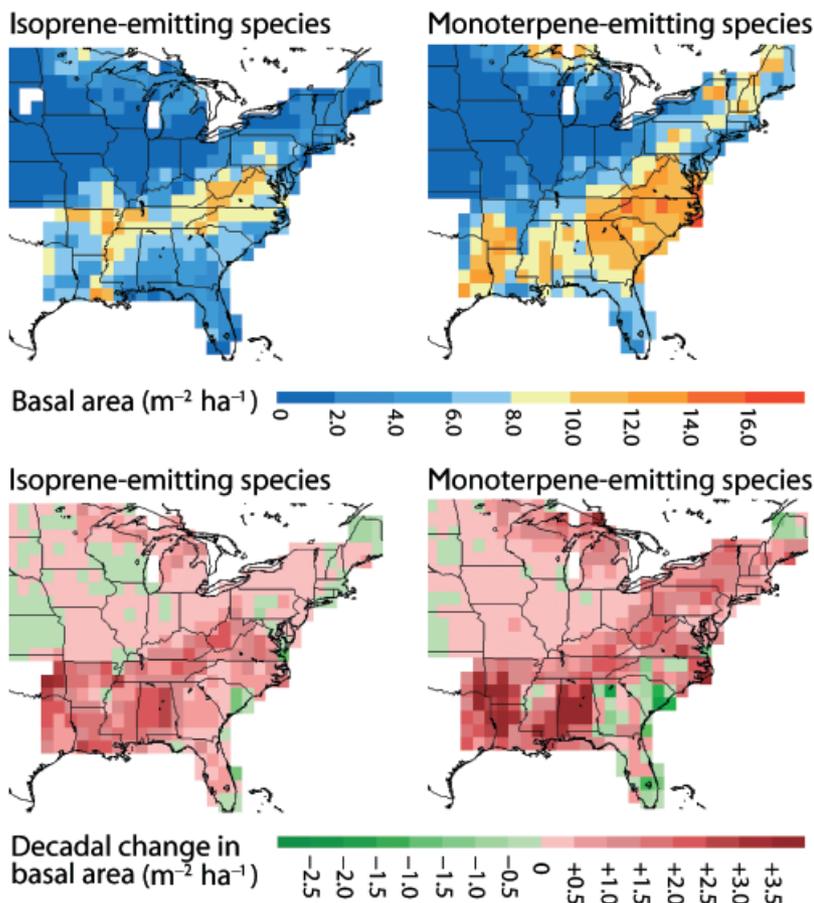

Fig. 1 (Top) Mid-1980s basal area of isoprene- and monoterpene-emitting tree species (m^2 ha^{-1}); (bottom) decadal change in basal areas (m^2 ha^{-1}). Calculated from the USDA Forest Service (FIA) inventory data. The values include differences in forest area.

basal area of monoterpene-emitting species was high in the Southern Appalachians and the Pinelands of the southeastern coastal plain (Pines tend to emit monoterpenes). Between the mid-1980s and the mid-1990s, there were systematic increases in the basal area of both isoprene- and monoterpene-emitting species, especially in the south of the region (Fig. 1, bottom). There were also some substantial decreases in the basal area of monoterpene-emitting species in South Carolina and Georgia (Fig. 1, bottom).

The detailed emission model was needed to provide quantitative estimates of BVOC emissions, and hence changes in BVOC emissions, from the inventory data. In a few locations, the model showed counterintuitive effects such as decreasing emissions where the basal area of emitters increased (this can occur for a number of reasons, e.g. where stand-level leaf area is already saturated and thus further increases in basal area do not increase leaf area), but these cases were rare and in general the predictions of the emissions model corresponded in a simple way to the patterns in the inventory data. The estimate of heatwave isoprene and monoterpene emission rates (Fig. 2) was strongly correlated with the pattern of standing basal area of isoprene- and monoterpene-emitting species (Fig. 1, top), and the estimated decadal change in BVOC emission rates (Fig. 3) was strongly correlated with the decadal change in basal area observed in the inventory data (Fig. 1, bottom).

Mid-1980s BVOC emission rates

The spatial pattern of estimated BVOC emissions was heterogeneous (Fig. 2), reflecting heterogeneity in the extent and species composition of forests (Fig. 1). The spatial distribution of emissions is in general agreement
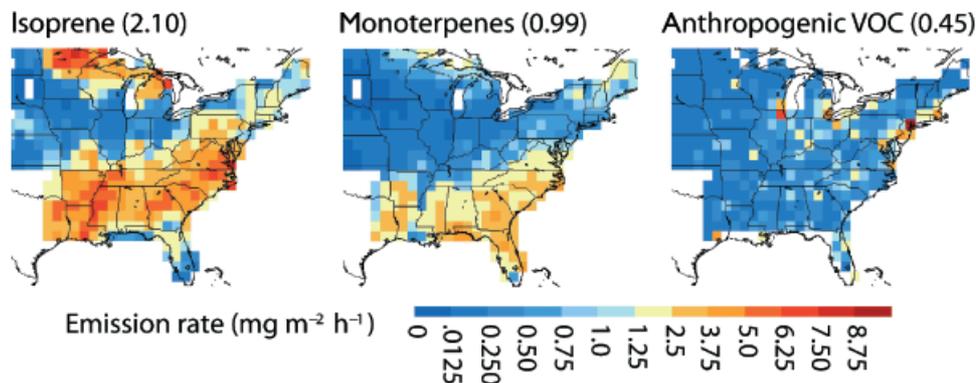

Fig. 2 Estimate of mid-1980s heatwave emission rates ($mg\,m^{-2}\,h^{-1}$) for isoprene and monoterpenes, compared with heatwave anthropogenic volatile organic compounds (VOC) emission rates. Anthropogenic emissions taken from the EPA AIRS data. Estimates from model B2 (Methods) driven with mid-1980s USDA Forest Service inventory data (FIA). Note the nonlinear scale. Average emission rate over all grid cells is given in parentheses above each map.
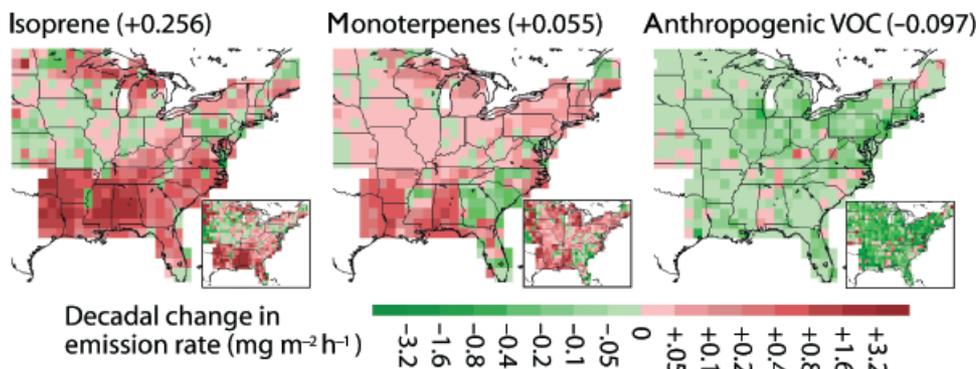

Fig. 3 Estimated decadal change in heatwave emission rate mid-1980s to mid-1990s ($mg\,m^{-2}\,h^{-1}$, per decade) for isoprene and monoterpenes, compared with decadal change in anthropogenic volatile organic compounds (VOC) emissions. Change estimate given by model B2 (Methods) driven separately with mid-1980s and mid-1990s USDA Forest Service inventory data (FIA). Anthropogenic emissions taken from the EPA AIRS data. Note nonlinear scale. Insets give percentage changes (scale from −30% to +30% decadal change). Average change in emission rate over all grid cells is given in parentheses above each map.

with previous estimates for the region and period, which used genus-level emission factors in combination with some satellite data, and some inventory data, to produce emission characteristics based on broad forest types (e.g. Kinnee *et al.*, 1997; Pierce *et al.*, 1998). The magnitude of our estimated heatwave isoprene emission rates are close to the most detailed previous estimate for the region (Kinnee *et al.* (1997): cf. Fig. 2 with plate 2 top in Kinnee *et al.* (1997): the emission units are the same, but our heatwave condition is slightly hotter and brighter). Our July average emissions (calculated from July 1990 climate data interpolated from ECMWF data: not shown) are slightly lower than BEIS-2, which is around half the GEIA estimate (Palmer *et al.*, 2003 and references therein). Heatwave BVOC emissions are estimated to have been considerably greater than heatwave AVOC emissions (Fig. 2: AVOC emission data taken from the EPA AIRS program: see http://www.epa.gov/air/data/goesel.html), although this comparison needs to be treated with some caution because of the light and temperature sensitivity of BVOC emissions.

The estimate given in Fig. 2 is from model B2, which we consider to be the most biologically reasonable of our six alternative emissions models B1–C3 (see Methods). The emission estimates were not too sensitive to the choice of these six options: the emission rates were in the order C3>B3>B1 ≈ B2 ≈ C1 ≈ C2, with models B1, C1, and C2 giving maps that were almost indistinguishable from model B2 (not shown). Models B3 and C3 differ from the others because they fix the LAI of each tree (at 6.0), thus stand-level LAI is either completely fixed (C3), or depends only on the extent to which tree crowns fill horizontal space (B3), which in both cases increases the estimated leaf area (and hence emissions) compared with the other models. Model C3 is particularly unrealistic because it assumes that in all stands, the canopy is perfectly filled and the LAI is 6.0: it was included here as a bounding case to test the robustness of the predictions.

Changes in BVOC emission rates

Our BVOC emission model translated the systematic changes in forest structure and composition recorded in the FIA data (Fig. 1) into quantitative estimates of the change in BVOC emission rates: the result was an estimation of rapid increases in emissions from the 1980s to the 1990s for both isoprene and monoterpenes (Fig. 3). Half of the grid cells covered by our analysis had decadal changes in heatwave isoprene emissions outside the range −2.3% to +16.8% with a corresponding range for monoterpenes of 0.2–17.1% (Fig. 3, insets). Although the percentage changes in AVOC emissions

were of a similar magnitude (half of the grid cells outside the range −28.7% to −5.1%), the 1980s heatwave emissions of BVOCs were greater (Fig. 2), thus the same percentage change in BVOC emissions was greater in absolute terms than the change in AVOC emissions.

This conclusion was relatively robust to the choice of the six alternative models B1–C3: five of the models gave maps of decadal changes in isoprene emissions that were visually indistinguishable from each other (not shown), and the outlying model (C3, the only model with no mechanisms for changes in total leaf area within a plot) gave decreases over much of the region where the other models gave increases. Crucially, however, the region of rapid increases in isoprene emissions in the southeast was common to all six models, as expected from the clear landscape-level increase in isoprene emitting species in that region (Fig. 1). For monoterpene emissions, five of the models gave maps of changes indistinguishable from each other, and the outlying model (C3) gave rapid *decreases* in the southeast. This is because many of the forests in this region were increasing rapidly in leaf area during this period. Model C3 cannot capture this effect, but is dominated by changes in forest area and changes in species composition, both of which acted to decrease monoterpene emissions in that region (Fig. 4). The data used to produce Fig. 3, and the discussion following, are from model B2.

Comparison with changes in AVOC emissions

The increases in heatwave BVOC emissions are estimated to have exceeded the decreases in heatwave AVOC emissions during the same period, as shown by the ratio of the changes in Fig. 3: averaged over all the grid cells in the region, the antilog of the mean of $\log(|\Delta BVOC|/|\Delta AVOC|)$ was 3.21, with 95% confidence interval 2.45–4.19. This means that for an average grid cell, the long-term change in heatwave BVOC emissions (usually an increase) was three times greater than the long-term change in heatwave AVOC emissions (usually a decrease). In the deep south region defined by Alabama, Arkansas, Louisiana, and Mississippi, the estimated difference was very large, with an average ratio of 29.0 (confidence interval 20.6–40.7), although there were also some regions where changes in AVOC emissions were greater than changes in BVOC (e.g. around New York City).

The estimated difference between BVOC and AVOC emissions, and hence any estimate of changes in emissions, depends on the choice of meteorological conditions, because BVOC emission rate is sensitive to meteorological conditions but AVOC emission rates are
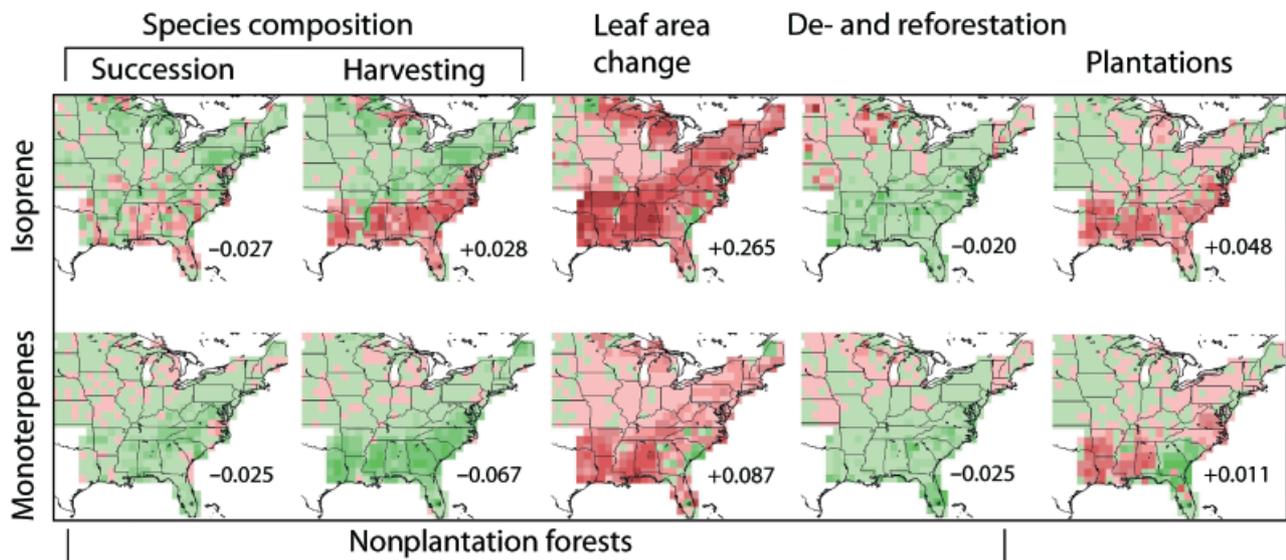
Fig. 4 Decadal change in heatwave isoprene and monoterpene emissions in the mid-1980s to mid-1990s ($mg\,m^{-2}\,h^{-1}$, per decade) caused by five separate processes. The average of the grid-cell decadal changes is given for each process by each map. Calculated from model B2 (Methods) in conjunction with the USDA Forest Service inventory data (FIA). Scale as in Fig. 3.

close to constant. We present results for heatwave conditions because these are important for peak O_3 events. Using our emission model to calculate emissions from hourly climate data for July 1990 (ECMWF data interpolated to a $1° \times 1°$ grid) gave a July average isoprene emission rate of approximately one-quarter of the heatwave emission rate, and for monoterpenes the average emission rate is approximately half the heatwave emission rate (not shown). Therefore, the decadal change in July average BVOC emissions was close to the decadal change in AVOC emissions: but for O_3 production July average emissions are less relevant than heatwave emissions.

Causes of change: processes

The decomposition into processes revealed that outside the southeastern US, the net increases in isoprene emissions were because of large increases from leaf-area change, and smaller decreases from species compositional change caused by ecological succession and harvesting (Fig. 4). In the southeastern US, the mix of processes was more complex (Fig. 4). Here, species composition change because of selective harvesting (mainly of pines) acted to increase isoprene but decrease monoterpene emissions. Ecological succession acted in the same direction at some locations, but in others it decreased isoprene emissions. There were substantial effects of plantation management, which increased both isoprene and monoterpene emissions in the deep south but increased isoprene and decreased

monoterpene emissions in South Carolina and Georgia. There was also a general increase in emissions because of leaf-area increases. Over the eastern US as a whole, changes in forest area were much less important than changes in the structure and species composition within established forests (Fig. 4).

Causes of change: species

In any one location, the changes in BVOC emissions resulted from changes in a small number of species. Figure 5 gives a detailed breakdown of the species-specific patterns from two regions that underwent rapid changes in BVOC emissions: South Carolina and Georgia (SC and GA), and the deep south (defined here as Alabama, Arkansas, Louisiana, and Mississippi). As Fig. 5 shows, in both cases the rapid increases in isoprene emissions were caused almost entirely by Sweetgum (*Liquidambar styraciflua*), which in both regions increased in both natural forests (defined here as non-planted forests), and in pine plantations. The decrease in monoterpene emissions in SC and GA was caused by a loss of several pine species from natural forests (from harvesting and succession, Fig. 4), and by loss of slash pine (*Pinus elliotii*) from pine plantations. The increase in monoterpene emissions in the deep south was because of an increase in loblolly pine (*P. taeda*), both in pine plantations and in natural forests. In addition, there were some smaller effects from Oak species (*Quercus*) in both regions, most notably the increase in isoprene emissions from Water Oak (*Quercus*
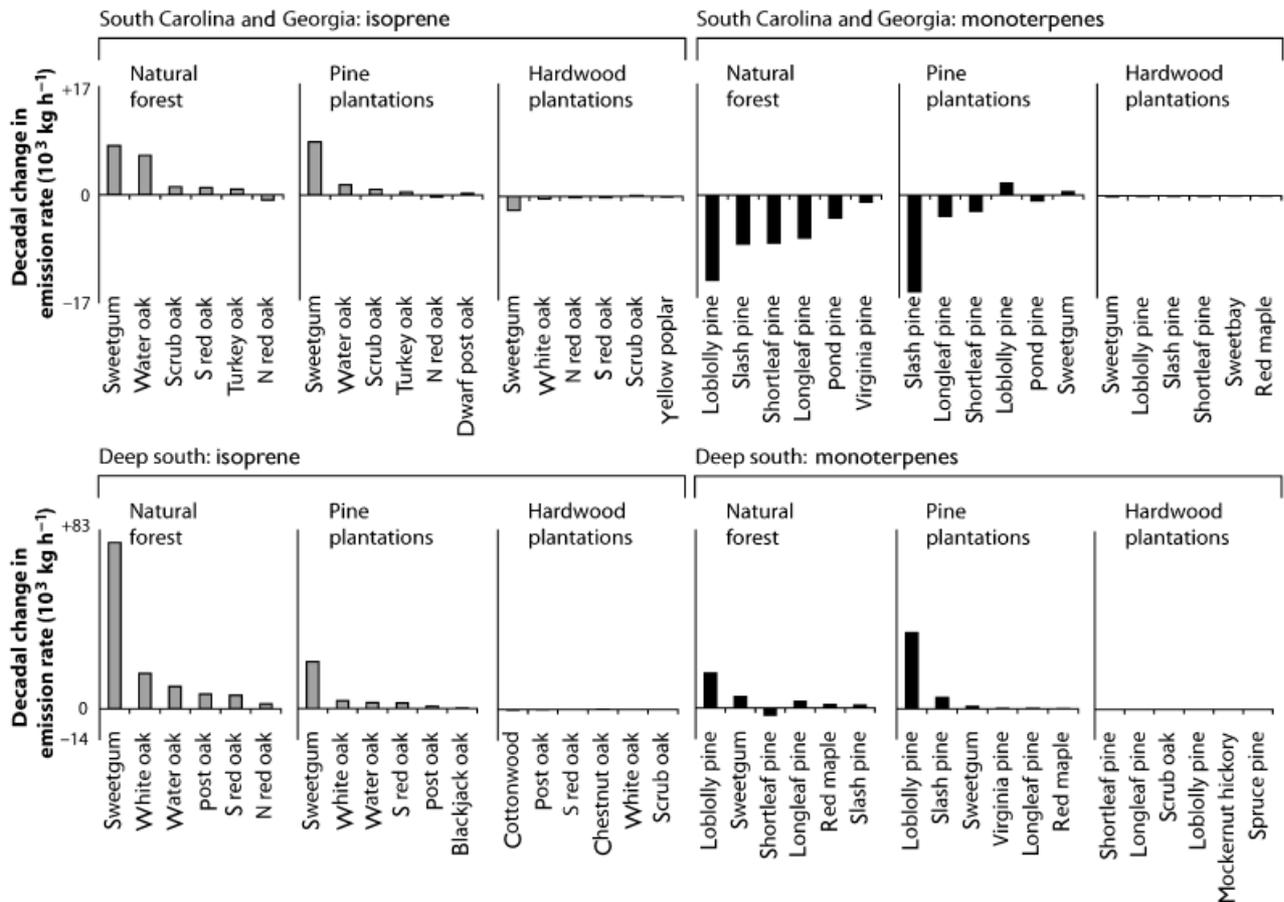
Fig. 5 Decadal change in heatwave emissions in the mid-1980s to mid-1990s of isoprene (grey bars) and monoterpene (black bars) caused by changes in individual species in different settings (natural forest, pine plantation, or hardwood plantation – see Methods), for two different regions, South Carolina and Georgia, and the deep south (defined here as Alabama, Arkansas, Louisiana, and Mississippi). Calculated from model B2 (Methods) in conjunction with the USDA Forest Service forest inventory data (FIA).

nigra) in SC and GA. Outside these regions (not shown), different species were important; e.g. the increases in isoprene emissions in Michigan and Wisconsin were because mainly to increases in the cover of two Aspens (Quaking and Bigtooth) and one Oak (Northern Red).

Discussion

Rapid changes in BVOC emissions

Our analysis suggests that between the 1980s and 1990s, a number of different factors combined to cause large changes in BVOC emissions (Fig. 2), including some very rapid increases in isoprene emissions across the southeastern US. The most important process was increasing forest leaf area (Fig. 4), which is estimated to have occurred because the basal area of VOC-emitting trees increased (Fig. 1 bottom). In any one location, these basal area changes reflected the interaction

between a number of different anthropogenic and autonomous processes affecting different species (e.g. Fig. 5), but they also reflect a general increase in basal area across the region during this period, due in large part to historical changes in land use and management. Whatever the cause of the increases, BVOC emissions may be expected to increase until leaf area approaches equilibrium with disturbance, at which point change in species composition is likely to become the dominant process driving BVOC emissions.

Like the legislated changes in AVOC emissions, most of the changes in BVOC emissions were caused by people. Harvesting and plantation management are obviously direct anthropogenic processes. Leaf area increases were caused by the increases in the total basal area of trees, which was because of some combination of changes in land use, harvesting, and anthropogenic CO_2 or other pollution. Ecological succession, although a natural process, was and is occurring so widely

mainly because forests are recovering from anthropogenic disturbance, and the direction of succession is affected and often dominated by anthropogenic influences including fire suppression, pollution, changes in the density of large herbivores (which themselves are mostly because of changes in hunting), and the treatment of land prior to abandonment. However, some of the changes observed in the inventory data could have been caused by natural process, for example storms or pest outbreaks. The analysis presented here does not allow the calculation of the relative importance of anthropogenic vs. natural change in eastern US forests, because it uses observed changes, which reflect the sum of all processes. However prior knowledge suggests that humans are by far the most important agent of change in US forests.

Uncertainty

The estimated changes in BVOC emissions presented here result entirely from systematic observed changes in the FIA inventory data, but there are important sources of uncertainty, including model assumptions and input parameters (see Methods: the uncertainty in the inventory data itself is likely to be small in comparison, see Appendix). These uncertainties are inherent to any estimate of fluxes at the ecosystem scale, and call for caution in the interpretation of results, especially in this case in any application to air-quality management. Since the most important process driving the estimated emission increases was increased leaf area, it would be helpful to have external data on LAI changes, but this is problematic. The only source of data extensive and intensive enough is satellite data, but over the range of LAI values of interest here (typically 3–6), NDVI, which is used a predictor for LAI, is relatively insensitive to changes in LAI (Wang *et al.*, 2001), and convertion of NDVI to LAI requires modelling that is itself subject to data and model uncertainties (Wang *et al.*, 2001). As a result, the reported accuracy of NDVI-based LAI estimates for mesic forests is low, even within relatively homogenous regions where the relevant forest characteristics are already known (e.g. Franklin *et al.*, 1997; Chen *et al.*, 2002). Furthermore, the calculation of long-term trends in NDVI is complicated by orbit drift and other problems (Gutman, 1999). Therefore currently, satellite-based observations of LAI are probably not sufficiently accurate to corroborate or invalidate our estimates of changing LAI. Nonetheless, the most detailed available estimates of long-term NDVI changes for this region do indicate increases between the 1980s and 1990s (Hicke *et al.*, 2002; Slayback *et al.*, 2003).

Other sources of uncertainty in the model include the species-specific BVOC emission rates and the details of the functions that predict emissions for given meteorological conditions, both of which are improving rapidly. However, *in situ* flux measurements of BVOC emission rates (e.g. Karl *et al.*, 2003) are not available at sufficient intensity or over large enough regions to validate the predictions of BVOC emission models, to identify trends directly, or to evaluate improvements in predictive ability (although where the emission models have been tested directly the predictions can be close to observations, e.g. Guenther *et al.*, 1996; Lamb *et al.*, 1996). Analysis of satellite formaldehyde columns is a promising technique for estimating isoprene emissions (Abbot *et al.*, 2003; Palmer *et al.*, 2003), but this technique is uncertain at present. Until sufficient data for verification become available, the predictions of BVOC emission models, and hence the estimate of changes in emissions that we present here, should be viewed with caution. However, the direction, spatial distribution, and relative magnitude of the changes in BVOC emissions estimated here are likely to be robust, because the systematic changes in the forest inventory data are so clear (Fig. 1) and statistically significant (Appendix). The most important uncertainties concern the exact magnitude of emission rates, and the magnitude of the changes.

Plantation forestry

Plantation forestry is estimated to have caused substantial changes in BVOC emissions in the southeast, as a result both of changes in the plantation species themselves (especially Loblolly pine), and in one interesting and important example, a species that comes to associate with plantations: sweetgum (*Liquidambar styraciflua*), which often appears in pine plantations in the south, and which in South Carolina and Georgia increased significantly within pine plantations (although sweetgum also increased in nonplantation forests all across the southeast: Fig. 5). It is interesting that this plantation system is comprised of two species that are very high emitters of the two main BVOCs. In addition, plantation management is improving continually, especially in the southeastern US, and this is likely to increase emissions independent of the changes captured in our analysis. For example fertilization of southern pine plantations increased from $16\,200\,\text{ha}\,\text{yr}^{-1}$ in 1988 to $344\,250\,\text{ha}\,\text{yr}^{-1}$ in 1998 (Johnsen *et al.*, unpublished): if this trend continues, it can be expected to increase tree growth rates and LAI, and so BVOC emissions.

The importance of plantation forestry to the BVOC emissions changes is especially relevant because

plantation forestry has increased greatly over the last few decades, and is set to continue increasing (Zhou et al., 2003), and because large increases in plantation forestry in the US and elsewhere have been suggested as part of strategies to offset carbon emissions, via carbon sequestration and/or biofuel production (e.g. Wright et al., 2000; Schneider & McCarl, 2003). The tree species proposed for use in these operations are high emitters for isoprene or monoterpenes (e.g. Poplars, Eucalypts, Sweetgum, Willows, Pines). Our results call for some caution in increasing plantation area because of increases in BVOC emissions, which may affect O_3 concentrations. It is possible that in some areas the air-quality considerations will be serious enough to tip the balance in favour of systems that do not use woody plants at all (e.g. biofuel systems based on switchgrass or annual crops: Schneider & McCarl, 2003), but this would depend on the complex interactions between NO_x, AVOCs, BVOCs, and the transport of various chemical species, which together determine O_3 concentrations: e.g. it is possible that increases in BVOC emissions would not have a significant effect on O_3 concentrations, or that the increases in BVOC emissions could be so large as to actually decrease O_3 (Roselle, 1994; Kang et al., 2003). Chemistry and transport models, together with economic analyses, are needed to address this issue.

Consequences for tropospheric O_3

BVOCs are known to act as precursors of tropospheric O_3, suggesting that the increases in BVOC emission rates estimated here are likely to have increased tropospheric O_3 concentrations, but this is not inevitable. For example, much of the increased isoprene emission was in relatively rural areas where NO_x emissions are low and O_3 production is less sensitive to VOC (NRC, 1991). In the southeastern US, a recent study has demonstrated that isoprene emission rates can already be great enough, and NO_x emissions low enough, for further increases in isoprene to decrease O_3 concentrations (Kang et al., 2003). To provide quantitative estimates of the changes in O_3 concentrations caused by changes in BVOC emission rates requires the use of a chemical transport model (e.g. Roselle, 1994; Horowitz et al., 1998; Pierce et al., 1998). However, our results do suggest that changes in BVOC emissions have been similar or greater than changes in AVOC emissions over the same period, which calls for increased attention to changes in BVOC emissions in modelling studies that assess the effects of recent and anticipated future changes in O_3 precursors (e.g. Tao et al., 2003). Importantly, the changes in BVOC emissions were inadvertent, unlike the deliberate decreases in AVOC emission achieved via EPA regulations over the same period (EPA, 2000). Overall, the results call for a wider recognition that O_3 production, and attempts to control O_3 precursors, occur within the context of disturbed, and hence dynamic biological landscape.

References

Abbot DS, Palmer PI, Martin RV et al. (2003) Seasonal and interannual variability of North American isoprene emissions as determined by formaldehyde column measurements from space. Geophysical Research Letters, 30, d.o.i.: 10.1029/2003GL017336.

Andreae M, Crutzen P (1997) Atmospheric aerosols: biogeochemical sources and role in atmospheric chemistry. Science, 276, 1052–1058.

Chojnacky DD (1998) Research Paper RMRS-4P-7. USDA Forest Research Service Rocky Mountain Research Station.

Chen JM, Pavlic G, Brown L et al. (2002) Derivation and validation of Canada-wide coarse-resolution leaf area index maps using high-resolution satellite imagery and ground measurements. Remote Sensing of Environment, 80, 165–184.

Collins WJ, Derwent RG, Johnson CE et al. (2002) The oxidation of organic compounds in the troposphere and their global warming potentials. Climatic Change, 52, 453–479.

Constable JVH, Guenther AB, Schimel DS et al. (1999) Modelling changes in VOC emissions in response to climate change in the continental United States. Global Change Biology, 5, 791–806.

EPA (2000) National air pollution emission trends 1900–1998. EPA-454/R-00-002.

Fiore AM, Jacob DJ, Bey I et al. (2002) Background ozone over the united states in summer: origin, trend and contribution to pollution episodes. Journal of Geophysical Research – Atmospheres, 107, d.o.i.: 10.1029/2002GL015601.

Franklin SE, Lavigne MB, Deuling MJ et al. (1997) Estimation of forest Leaf Area Index using remote sensing and GIS. International Journal of Remote Sensing, 18, 3459–3471.

Fuentes JD, Lerdau M, Atkinson R et al. (2000) Biogenic hydrocarbons in the atmospheric boundary layer: a review. Bulletin of the American Meteorological Society, 81, 1537–1575.

Guenther AB, Zimmerman P, Harley PC et al. (1993) Isoprene and monoterpene emission rate variability – model evaluation and sensitivity analyses. Journal of Geophysical Research – Atmospheres, 98, 12609–12617.

Guenther AB, Zimmerman P, Wildermuth M (1994) Natural volatile organic compound emission rate estimates for United States woodland landscapes. Atmospheric Environment, 28, 1197–1210.

Guenther A, Greenberg J, Harley P et al. (1996) Leaf, branch, stand and landscape scale measurements of volatile organic

compound fluxes from US woodlands. *Tree Physiology*, **16**, 17–24.

Guenther AB, Geron C, Pierce T *et al.* (2000) Natural emissions of non-methane volatile organic compounds; carbon monoxide, and oxides of nitrogen from North America. *Atmospheric Environment*, **34**, 2205–2230.

Gutman GG (1999) On the use of long-term global data of land reflectances and vegetation indices derived from the advanced very high resolution radiometer. *Journal of Geophysical Research*, **104**, 6241–6255.

Hansen MH, Frieswyck T, Glover JF *et al.* (1992) *USDA Forest Service General Technical Reports*, NC-151.

Harley P, Guenther A, Zimmerman P (1997) Environmental controls over isoprene emission in deciduous oak canopies. *Tree Physiology*, **17**, 705–714.

Harley PC, Monson RK, Lerdau MT (1999) Ecological and evolutionary aspects of isoprene emissions from plants. *Oecologia*, **118**, 109–123.

Hayden BP (1998) Ecosystem feedbacks on climate at the landscape scale. *Philosophical Transactions of the Royal Society of London*, **352B**, 5–18.

Hesstvedt E, Isaksen ISA, Hov O (1978) Ozone generation over rural areas. *Environmental Science and Technology*, **12**, 1279–1284.

Hicke JA, Asner GP, Randerson JT *et al.* (2002) Trends in North American net primary productivity derived from satellite observations, 1982–1998. *Global Biogeochemical Cycles*, **16**, d.o.i.: 10.1029/2001GB001550.

Horowitz LW, Liang JY, Gardner JM *et al.* (1998) Export of reactive nitrogen from North America during summertime: sensitivity to hydrocarbon chemistry. *Journal of Geophysical Research – Atmospheres*, **103**, 13451–13476.

Hurtt GC, Pacala SW, Moorcroft PR *et al.* (2002) Projecting the future of the U.S. carbon sink. *Proceedings of the Natural Academy of Sciences USA*, **99**, 1389–1394.

Jacob DJ (1999) *Introduction to Atmospheric Chemistry*. Princeton University Press, NJ, USA.

Kang DW, Aneja VP, Mathur R *et al.* (2003) Nonmethane hydrocarbons and ozone in three rural southeast United States national parks: a model sensitivity analysis and comparison to measurements. *Journal of Geophysical Research – Atmospheres*, **108**, d.o.i.: 10.1029/2002JD003054.

Karl T, Guenther A, Spirig C *et al.* (2003) Seasonal variation of biogenic VOC emissions above a mixed hardwood forest in northern Michigan. *Geophysical Research Letters*, **30**, d.o.i.: 10.1029/2003GL018432.

Kesselmeier J, Staudt M (1999) Biogenic volatile organic compounds (VOC): an overview on emission, physiology and ecology. *Journal of Atmospheric Chemistry*, **33**, 23–88.

Kinnee E, Geron C, Pierce T (1997) United States land use inventory for estimating biogenic ozone precursor emissions. *Ecological Applications*, **7**, 46–58.

Lamb B, Pierce T, Baldocchi D *et al.* (1996) Evaluation of forest canopy models for estimating isoprene emissions. *Journal of Geophysical Research – Atmospheres*, **101**, 22787–22979.

Leaitch WR, Bottenheim TA, Biesenthal TA *et al.* (1999) A case study of gas-to-particle conversion in an eastern Canadian forest. *Journal of Geophysical Research – Atmospheres*, **104**, 8095–8111.

Lerdau MT, Slobodkin L (2002) Trace gas emissions and species-dependent ecosystem services. *Trends in Ecology and Evolution*, **17**, 309–312.

Lin CYC, Jacob DJ, Fiore AM (2001) Trends in exceedances of the ozone air quality standard in the continental United States 1980–1998. *Atmospheric Environment*, **35**, 3217–3228.

Mäkelä JM, Aalto P, Jokinen V *et al.* (1997) Observations of ultrafine aerosol particle formation and growth in boreal forest. *Geophysical Research Letters*, **24**, 1219–1222.

Martin GL (1982) A method for estimating ingrowth on permanent horizontal sample points. *Forest Science*, **28**, 110–114.

Mickley LJ, Jacob DJ, Rind D (2001) Uncertainty in preindustrial abundance of tropospheric ozone: implications for radiative forcing calculations. *Journal of Geophysical Research – Atmospheres*, **106**, 3389–3399.

Monson RK, Lerdau MT, Sharkey TD *et al.* (1995) Biological aspects of constructing volatile organic compound emission inventories. *Atmospheric Environment*, **29**, 2989–3002.

NRC (1991) *Rethinking the Ozone Problem in Urban and Regional Air Pollution*. National Academic Press, Washington, DC, USA.

Pacala SW, Canham CD, Saponara J *et al.* (1996) Forest models defined by field measurements: estimation, error analysis and dynamics. *Ecological Monographs*, **66**, 1–43.

Palmer PI, Jacob DJ, Fiore AM *et al.* (2003) Mapping isoprene emissions over North America using formaldehyde column observations from space. *Journal of Geophysical Research*, **108**, 4180.

Phillips DL, Brown SL, Schroeder PE *et al.* (2000) Toward error analysis of large-scale forest carbon budgets. *Global Ecology and Biogeography*, **9**, 305–313.

Pierce T, Geron C, Bender L *et al.* (1998) Influence of increased isoprene emissions on regional ozone modelling. *Journal of Geophysical Research – Atmospheres*, **103**, 25611–25629.

Reagan RW (1980) 'Approximately 80 percent of our air pollution stems from hydrocarbons released by vegetation. So let's not go overboard in setting and enforcing tough emission standards for man-made sources', quoted in *Sierra Magazine*, September 10.

Roselle SJ (1994) Effects of biogenic emission uncertainties on regional photochemical modelling of control strategies. *Atmospheric Environment*, **28**, 1757–1772.

Sanderson MG, Jones CD, Collins WJ *et al.* (2003) Effect of climate change in isoprene emissions and surface ozone levels. *Geophysical Research Letters*, **30**, d.o.i.: 10.1029/2003GL017642.

Schneider UA, McCarl BA (2003) Economic potential of biomass based fuels for greenhouse gas emission mitigation. *Environmental and Resource Economics*, **24**, 291–312.

Seinfeld JH, Pandis SN (1998) *Atmospheric Chemistry and Physics: from Air Pollution to Climate Change*. Wiley, New York, USA.

Shallcross DE (2000) A role for isoprene in biosphere–climate–chemistry feedbacks. *Atmospheric Environment*, **34**, 1659–1660.

Sillman S (1999) The relation between ozone, NO_x and hydrocarbons in urban and rural polluted environments. *Atmospheric Environment*, **33**, 1821–1845.

Slayback DA, Pizon JE, Sietseo OL *et al.* (2003) Northern hemisphere photosynthetic trends 1982–1999. *Global Change Biology*, **9**, 1–15.

Stewart H, Hewitt CN, Bunce RGH *et al.* (2003) A highly spatially and temporally resolved inventory for biogenic isoprene and monoterpene emissions: model description and application to Great Britain. *Journal of Geophysical Research – Atmospheres*, **108**, d.o.i.: 10.1029/2002JD002694.

Tao Z, Larson SM, Wuebbles AW *et al.* (2003) A summer simulation of biogenic contributions to ground-level ozone over the continental United States. *Journal of Geophysical Research – Atmospheres*, **108**, d.o.i.: 10.1029/2002JD002945.

Ter-Mikaelian MT, Korzukhin MD (1997) Biomass equations for sixty-five North American tree species. *Forest Ecology and Management*, **97**, 1–24.

Wang K-Y, Shallcross DE (2000) Modelling terrestrial biogenic isoprene fluxes and their potential impact on global chemical species using a coupled LSM-CTM model. *Atmospheric Environment*, **34**, 2909–2925.

Wang YJ, Tian YH, Zhang Y *et al.* (2001) Investigation of product accuracy as a function of input and model uncertainties – case study with SeaWiFS and MODIS LAI/FPAR algorithm. *Remote Sensing of Environment*, **78**, 299–313.

White MA, Thornton PE, Running SW *et al.* (2000) Parameterization and sensitivity analysis of the BIOME-BGC terrestrial ecosystem model: net primary production controls. *Earth Interactions*, **4**, 1–85.

Wiedinmyer C, Friedfeld S, Baugh W *et al.* (2000) Measurement and analysis of atmospheric concentrations of isoprene and its reaction products in central Texas. *Atmospheric Environment*, **35**, 1001–1013.

Wright JA, DiNicola A, Gaitan E (2000) Latin American forest plantations: opportunities for carbon sequestration, economic development and financial returns. *Journal of Forestry*, **98**, 20–23.

Zhou XP, Mills JR, Teeter L (2003) Modelling forest type transitions in the southcentral region: results from three models. *Southern Journal of Applied Forestry*, **27**, 190–197.

Appendix: Error analysis for the FIA data

Our estimates of changes in the rate of VOC emissions (Fig. 3) depend on the reliability of the measured changes in stand structure and composition (Fig. 1). In this appendix, we examine the magnitude of uncertainty in the FIA data and assess the robustness of our estimates to this uncertainty. Our conclusion is that the estimates presented in this paper are robust to the level of uncertainty in the FIA data.

Changes in basal area of emitting species

First, we present a very simple analysis of grid-cell level changes in the basal area of emitting species between the two FIA survey dates (Fig. 1). We classified each species in the FIA as emitting or nonemitting for isoprene and monoterpenes, defined, respectively, as potential leaf-level emission greater or less than 1.0 mg

(isoprene) g^{-1} (leaf dry weight) h^{-1}. A total basal area of isoprene/monoterpene emitters, $B_{\mathrm{iso/mono}}^{(j,t)}(\mathrm{cm}^2\,\mathrm{ha}^{-1})$, is then calculated for each plot j at time t:

$$B_{\mathrm{iso}}^{(j,t)} = \sum_{\{i \in \mathrm{RB}_{\mathrm{iso/mono}}(j)\}} \pi\, w^{(i)}[\mathrm{dbh}^{(i,t)}/2]^2, \qquad (A1)$$

where $\mathrm{dbh}^{(i,t)}$ is the diameter at breast (cm) height of tree i at time t; $w^{(i)}$ is the tree expansion factor defined in Methods; and the set $\mathrm{RB}_{\mathrm{iso}}(j)$ contains all isoprene-emitting trees within plot j, excluding as before trees greater than 5 in (12.7 cm) in diameter that were not measured in the first inventory (following Martin, 1982). A rate of change of isoprene-emitting species, $\Delta B_{\mathrm{iso/mono}}^{(j)}(\mathrm{cm}^2\,\mathrm{ha}^{-1}\,\mathrm{yr}^{-1})$, is then calculated for each plot:

$$\Delta B_{\mathrm{iso}}^{(j)} = [1/\Delta t][B_{\mathrm{iso/mono}}^{(j,t+\Delta t)} - B_{\mathrm{iso/mono}}^{(j,t)}], \qquad (A2)$$

where Δt (decades) is the period between the FIA surveys. A grid-cell level average change mid-1980s basal area of isoprene emitting species, $B_{\mathrm{iso/mono}}^{(k)}$, is given by a weighted mean of the plot-level values:

$$B_{\mathrm{iso/mono}}^{(k)} = \frac{\sum_{\{j \in R_1(k)\}} w^{(j)} B_{\mathrm{iso/mono}}^{(j)}}{\sum_{\{j \in R_1(k)\}} w^{(j)}}, \qquad (A3)$$

where the set $R_1(k)$ contains all plots within grid cell k that have data from the first (mid-1980s) FIA survey, and $w^{(j)}$ is the plot expansion factor. A grid-cell decadal change in basal area, $\Delta B_{\mathrm{iso/mono}}^{(k)}$, is given by

$$\Delta B_{\mathrm{iso/mono}}^{(k)} = \frac{\sum_{\{j \in R_2(k)\}} w^{(j)} \Delta B_{\mathrm{iso/mono}}^{(j)}}{\sum_{\{j \in R_2(k)\}} w^{(j)}}, \qquad (A4)$$

where the set $R_2(k)$ is all plots within grid cell k that have data from both (mid-1980s and mid-1990s) FIA surveys. Figure 1 gives the values for $B_{\mathrm{iso/mono}}^{(k)}$ and $\Delta B_{\mathrm{iso/mono}}^{(k)}$. Over most of the region, the direction and spatial distribution of $B_{\mathrm{iso}}^{(k)}$ and $\Delta B_{\mathrm{iso}}^{(k)}$ is very similar to $I_{\mathrm{iso}}^{(k)}$ and $\Delta I_{\mathrm{iso}}^{(k)}$, i.e. the basic pattern of isoprene emission rates, and changes in those rates, is predicted by the much simpler analysis of changes in the basal area of emitters (cf. Fig. 1 with Figs 2 and 3). The few grid cells where $\Delta B_{\mathrm{iso}}^{(k)}$ and $\Delta I_{\mathrm{iso}}^{(k)}$ are opposite in direction are in regions where the estimated rate of change in isoprene emissions is small in magnitude. This suggests that in general the estimated direction of change in isoprene emissions is unlikely to be highly sensitive to different assumptions in the isoprene emission model (e.g. our different models B2–C3, or alternative emissions models BEIS1, BEIS2: Pierce *et al.*, 1998).

However, within the isoprene-emitting species (as defined here), there is over 100-fold variation in emission rates, so changes in species composition can lead to changes in isoprene emissions equal to or greater than those resulting from changes in basal area.

Furthermore, the dependency of spatial distribution of leaves on the basal area of individuals, and the nonlinearity of the Guenther *et al.* (1993) algorithms, introduce nonlinearities into the relationship between plot-level basal area and plot-level emissions. These features explain why the relative magnitude of the direction of changes in basal area of emitters does not correspond exactly to the magnitude of the changes in isoprene emissions.

Uncertainty in basal area changes

Double sampling for stratification (Chojnacky, 1998) involves two sources of uncertainty: the uncertainty associated with estimating the relative frequency of the various forest cover strata (as given by the plot-level expansion factors), and the uncertainty associated with estimating a mean value for each of the strata. The second source of uncertainty can be quantified directly from the FIA data by calculating the sample variance for each of the stratum means. The first source of uncertainty, however, cannot be quantified directly from the data provided on the FIA database because it does not include the first-phase sample sizes (i.e. the number of photo-interpreted points used to estimate the plot-level expansion factors). As a result, we cannot provide a direct estimate of the uncertainty for each of the 37 states included in our analysis. Nevertheless, based on a previous error analysis (Phillips *et al.*, 2000), we can provide an estimate of the level of uncertainty in five southeastern states. All sources of error in estimating changes in basal area are covered by Phillips *et al.* (2000), including the photo-point- dependent error due in estimating the relative frequency of different strata.

Following the error analysis presented in Phillips *et al.* (2000), the change in basal area observed in any state can be divided into the natural processes of growth and mortality $\Delta_{\mathrm{ngm}}B^{(\mathrm{state})}$, and harvesting $\Delta_{\mathrm{harv}}B^{(\mathrm{state})}$:

$$\Delta B^{(\mathrm{state})} = \Delta_{\mathrm{ngm}}B^{(\mathrm{state})} + \varepsilon(\mathrm{ngm, state})$$
$$- \Delta_{\mathrm{harv}}B^{(\mathrm{state})} + \varepsilon(\mathrm{harv, state}), \qquad (\mathrm{A5})$$

where $\varepsilon(\mathrm{ngm}, k)$ and $\varepsilon(\mathrm{harv}, k)$ are the errors associated with $\Delta_{\mathrm{ngm}}B^{(\mathrm{state})}$ and $\Delta_{\mathrm{harv}}B^{(\mathrm{state})}$. In Eqn (A5), $\Delta_{\mathrm{ngm}}B^{(\mathrm{state})}$ and $\Delta_{\mathrm{harv}}B^{(\mathrm{state})}$ are taken to be the true mean change in basal area associated with natural processes and harvesting, respectively, and $\Delta B^{(\mathrm{state})}$ is taken to be the estimate of these processes, which is subject to the error terms $\varepsilon(\mathrm{ngm, state})$ and $\varepsilon(\mathrm{harv, state})$. The difference between the estimate $\Delta B^{(\mathrm{state})}$ and the true net change in basal area $\Delta\hat{B}^{(\mathrm{state})}$ is given by the sum of the error terms:

$$\Delta B^{(\mathrm{state})} - \Delta\hat{B}^{(\mathrm{state})} = \varepsilon(\mathrm{ngm, state})$$
$$+ \varepsilon(\mathrm{harv, state}). \qquad (\mathrm{A6})$$

Phillips *et al.* (2000) gives the standard errors associated with the values for state-level estimates of $\Delta_{\mathrm{ngm}}B^{(\mathrm{state})}$ and $\Delta_{\mathrm{harv}}B^{(\mathrm{state})}$, as a percentage of the estimate, for each state. This means for example that if $\Delta_{\mathrm{ngm}}B^{(\mathrm{state})}$ takes the value 100.0 U and the standard error is 1.91%, the standard error associated with $\Delta_{\mathrm{ngm}}B^{(\mathrm{state})}$ is 1.91 U. 95% confidence intervals for $\Delta_{\mathrm{ngm}}B^{(\mathrm{state})}$ and $\Delta_{\mathrm{harv}}B^{(\mathrm{state})}$ are approximately twice these values. Importantly, the fact that the FIA re-measures exactly the same plots reduces the error associated with the estimates of changes, i.e. $\varepsilon(\mathrm{ngm, state})$ and $\varepsilon(\mathrm{harv, state})$, compared with what would be expected from a simple comparison of the errors on the absolute values at either time. This is because the dominant sources of error tend to increase or decrease the estimated values together, and thus the error tends to cancel when calculating a change. For example, Phillips *et al.* (2000) quote a standard error for the carbon stock at one time of 0.6% of the stock, but a standard error for the change in carbon stock of 0.06% of the stock (from Table 2 in Phillips *et al.* (2000), calculated by taking the standard error on the change in stock for all five states, and expressing as a percentage of the stock at time 1). This is in stark contrast to the simple expectation of summing the standard errors from the two stock estimates, which would suggest $2 \times 0.6 = 1.2\%$ error.

Table A1 applies this error analysis to values of $\Delta B_{\mathrm{iso}}^{(\mathrm{state})}$ (analogous to $\Delta B_{\mathrm{iso}}^{(k)}$, but calculated at the state level). A conservative estimate of the uncertainty on the ΔB_{iso} is given in Table A1, by assuming that the errors associated with both $\Delta_{\mathrm{ngm}}B$ and $\Delta_{\mathrm{harv}}B$ lay on their respective 95% confidence boundaries (the probability of both error terms being this far from the mean is approximately $0.05 \times 0.05 = 0.0025$). Even so, only one state has confidence intervals around ΔB_{iso} that contain zero, and this was South Carolina, which was approximately 50:50 increases and decreases at the state level (Fig. 1). The state-level increases in the basal area of isoprene emitters in the other states are therefore highly statistically significant.

While these increases are significant at the state level, the basal area of emitters has declined in certain areas within each of these states. For example the basal area of isoprene emitters decreased in several grid cells located on the coast of South Carolina. Though localized, such declines may be of interest; hence, we have presented our results at a resolution of $1° \times 1°$ to reveal the substate heterogeneity. However, the changes estimated for a particular grid cell may not be significant even though the overall changes are significant at the state level, because sampling error increases as the sample size decreases.

Because the standard error is inversely proportional to the sample size, we can expect the error terms to

Table A1 Error analysis for the changes in basal area of isoprene-emitting species in the five states analysed in Phillips *et al.* (2000)

	$\Delta_{\mathrm{ngm}}B_{\mathrm{iso}}^{(\mathrm{state})}$ ($\mathrm{cm^2\,ha^{-1}\,yr^{-1}}$)			$\Delta_{\mathrm{harv}}B_{\mathrm{iso}}^{(\mathrm{state})}$ ($\mathrm{cm^2\,ha^{-1}\,yr^{-1}}$)			$\Delta B_{\mathrm{iso}}^{(\mathrm{state})}$ ($\mathrm{cm^2\,ha^{-1}\,yr^{-1}}$)		
state	Estimate	Standard error (%)	95% Confidence interval	Estimate	Standard error (%)	95% Confidence interval	Estimate	Lower limit	Upper limit
FL	748.7	1.72	25.8	287.7	3.59	20.7	461.0	414.6	507.5
GA	1294.9	1.17	30.3	705.6	2.58	36.4	589.3	522.6	656.0
NC	1750.0	1.23	43.0	1021.1	3.68	75.1	728.7	610.7	847.1
SC	1078.0	4.14	89.2	993.9	3.63	72.1	83.0	−78.3	244.4
VA	2125.9	1.29	54.8	1244.7	4.65	115.8	881.2	710.6	1051.8

The upper and lower limits refer to the confidence intervals for $P = 0.0025$ (see the text). FL, Florida; GA, Georgia; NC, North Carolina; SC, South Carolina; VA, Virginia.

increase with respect to the figures quoted in Phillips *et al.* (2000) by a factor $\sqrt{n}$, where n is the number of grid cells within a state (because the number if plots in each cell is inversely proportional to n). For the region analysed in Phillips *et al.* (2000), the average value of n is 13.8; thus, on average over the southeastern region, the error in this region can be expected to increase by a factor $\sqrt{13.8} = 3.71$.

Repeating the calculations presented in Table A1 for the same five states at the level of the grid cell, with the standard error term within each grid cell increased by the factor $\sqrt{n}$, where n is the number of grid cells in the state, leaves the estimate of ΔB_{iso} in 30% of the grid cells as nonsignificant, that is, not significantly different from zero (although it should be noted that as before,

this estimate is very conservative because it uses 95% intervals on two terms, giving an approximate combined probability of $P = 0.0025$ as explained). Crucially, however, even if none of the within-cell changes were significantly different from zero, the marked spatial coherence in the direction and magnitude of the estimated changes in basal area within different cells (Fig. 1) is an extremely unlikely outcome of an underlying process that was random in direction or magnitude, and thus is itself a strong indication of statistical significance. Indeed, the spatial coherence in the direction and magnitude of the estimated changes is the reason that the results are significant at the state level in all five cases.